Molecular Therapy
Oncolytics
Original Article

Single-cell transcriptomics reveal *DHX9* in mature B cell as a dynamic network biomarker before lymph node metastasis in CRC

Huisheng Liu,[1,7] JiaYuan Zhong,[2,7] JiaQi Hu,[1] ChongYin Han,[1] Rui Li,[4] XueQing Yao,[5] ShiPing Liu,[6] Pei Chen,[2] Rui Liu,[2,3] and Fei Ling[1]

[1]School of Biology and Biological Engineering, South China University of Technology, 381 Wushan Road, Guangzhou, Guangdong 510641, China; [2]School of Mathematics, South China University of Technology, Guangzhou, Guangdong 510641, China; [3]Pazhou Lab, Guangzhou, Guangdong 510330, China; [4]Department of Pathology, Southern Medical University Nanfang Hospital, Guangzhou, Guangdong 510515, China; [5]Department of General Surgery, Guangdong Provincial People's Hospital, Guangdong Academy of Medical Sciences, School of Medicine, South China University of Technology, Guangzhou, Guangdong 510080, China; [6]Shenzhen Key Laboratory of Single-Cell Omics, BGI-Shenzhen, Shenzhen 518083, China

Increasing evidence indicates that mature B cells in the adjacent tumor tissue, both as an intermediate state, are vital in advanced colorectal cancer (CRC), which is associated with a low survival rate. Developing predictive biomarkers that detect the tipping point of mature B cells before lymph node metastasis in CRC is critical to prevent irreversible deterioration. We analyzed B cells in the adjacent tissues of CRC samples from different stages using the dynamic network biomarker (DNB) method. Single-cell profiling of 725 CRC-derived B cells revealed the emergence of a mature B cell subtype. Using the DNB method, we identified stage II as a critical period before lymph node metastasis and that reversed difference genes triggered by DNBs were enriched in the Janus kinase (JAK)-signal transducer and activator of transcription (STAT) pathway involving B cell immune capability. *DHX9* (DEAH-box helicase 9) was a specific para-cancerous tissue DNB key gene. The dynamic expression levels of *DHX9* and its proximate network genes involved in B cell-related pathways were reversed at the network level from stage I to III. In summary, *DHX9* in mature B cells of CRC-adjacent tissues may serve as a predictable biomarker and a potential immune target in CRC progression.

INTRODUCTION

Colorectal cancer (CRC) is the third most common cancer (6.1% incidence) and fourth most fatal cancer (9.2% mortality) in the world.[1] In next 10 years, CRC is expected to cause 2.2 billion new cases and 1.1 billion additional deaths.[2] Despite the development of imaging and surgical techniques and multimodal therapy, the overall survival rate of patients with advanced CRC remains low.[3,4] The 5-year survival rate for CRC is significantly lower in stages III and IV than in stages I and II.[5] Para-cancerous tissue is often used as a control in cancer research. However, it has been theorized that cancer formation is a process involving gradual accumulation of mutations. Paraneoplastic tissue, as an intermediate state, is a group of cells that are morphologically normal before tumor formation but have undergone alterations at the molecular level.[6,7] Transcriptomic studies have shown that large numbers of molecular and cellular events occur in para-cancerous tissues, including epithelial-mesenchymal transition (EMT), tumor necrosis factor (TNF)-α and transforming growth factor (TGF)-β signaling, and apoptosis.[8] In particular, the pro-inflammatory microenvironment of para-cancerous tissues is favorable for CRC progression.[9] The tumor immune microenvironment (TME) is considered to be a mixture of tumor cells, stromal cells, differentiated cells from hematopoietic stem cells, and non-cellular components.[10] Cross-talk in TME plays an important facilitating and inhibiting role in the progression of CRC.[11] In the TME, the targeting cytotoxic T lymphocyte antigen 4 (CTLA4) or programmed cell death 1 (PD1) pathway can effectively improve patient survival.[12–15] The para-cancerous tissue microenvironment is not only essential for the normal physiological and biological behavior of an organ but is also critical in opposing resistance to malignant cell growth.[16] Our previous studies have shown that microbiome dysbiosis is significant in the para-cancerous tissue of CRC during metastasis.[17] However, the role of immune cells and others in the para-cancerous microenvironment and the underlying mechanism in tumor progression are unclear.

B cells (bursal-derived lymphocytes) are the major population of immune cells in the TME that execute the humoral immunity in cancer metastasis.[18] B cells mature in the bone marrow or lymph node.[19] Mature B cells play a positive role in tumor immunity and home

Received 6 February 2021; accepted 8 June 2021;
https://doi.org/10.1016/j.omto.2021.06.004.

[7]These authors contributed equally

Correspondence: Liu Rui, School of Mathematics, South China University of Technology, Guangzhou, Guangdong 510641, China.
E-mail: scliurui@scut.edu.cn
Correspondence: Fei Ling, School of Biology and Biological Engineering, South China University of Technology, 381 Wushan Road, Guangzhou 510641, China.
E-mail: fling@scut.edu.cn

to sites of infection or inflammation.[20] More importantly, mature B cells can perform antigen presentation and then proliferate and differentiate into plasma cells and memory cells with the assistance of helper T cells.[21] Thus, mature B cells are positively immune to CRC through antigen presentation, development, and migration. For instance, the Janus kinase (JAK)-signal transducer and activator of transcription (STAT) signaling pathway, under the influence of immune factors, plays an important role in B cell development, and any changes in its activity can affect tumor progression.[22,23] Many studies have shown that tumor-infiltrating B cells (TIL-Bs) in the TME of CRC may be plausible tumor biomarkers and potential targets for CRC immunotherapy.[24,25] In addition, mature B cells in adjacent tissues, under the action of chemokines (CCR2 and CCR7), metastasize to tumor tissues to exercise their functions such as induction in the lymph node and interaction with antigen-presenting cells (APCs).[26,27] At the same time, deficiency of mature B cells has been shown to increase tumor growth in mouse models.[20] Therefore, dynamic changes in the immune activity of mature B cells in para-cancerous tissues may influence tumor progression, especially during early stages of CRC.[6,8] Thus, it is important to capture this change in para-cancerous mature B cells at an early stage of CRC (before lymph node metastasis) to prevent cancer progression and uncover important biomarkers to provide new immune targets and prognostic indicators.

B cell antigen presentation and B cell development during CRC progression are dynamic processes.[28] The metastasis of CRC is preceded by a transitional phase characterized by dramatic changes in the immune activity of B cells, which play an important role in the metastasis of CRC.[29] To quantify this process, we applied dynamic network biomarkers (DNBs)[29–31] to predict the tipping point for CRC metastasis. DNBs are a group of strongly correlated and fluctuating molecules used for disease prediction or as an early warning. Unlike differentially expressed genes (DEGs), which are molecular biomarkers primarily used to detect disease status,[32] DNBs are used for detecting pre-mutation critical signals in disease and provide a new perspective for accurately predicting CRC metastasis and uncovering potential therapeutic targets.[33–35] Quantification of the dynamics of immunoreactivity of mature B cells in CRC progression by the DNB method may allow prediction of the most critical time points for early intervention and discovery of B cell-related immunotherapy targets and prognostic markers.

In this study, we used DNB analysis at the single-cell transcriptome level to evaluate gene network changes in mature B cells from CRC-adjacent tissues and predict the critical period of lymph node metastasis before CRC stage II (the following stages are American Joint Committee on Cancer [AJCC] tumor-lymph node-metastasis [TNM] stages). We also explain the reasons for stage II being a critical period in terms of network level and immune function, especially the JAK-STAT signaling pathway. We finally obtained DEAH-box helicase 9 (*DHX9*), a key DNB gene, as a biomarker in adjacent tissues B cells that is indicative of pre-metastasis before lymph node metastasis and could be used as a potential immunotherapy target.

RESULTS

B cell atlas revealed a mature B cell subtype in CRC

We performed single-cell RNA sequencing (Smart-Seq2) on immune cells ($CD45^+$) isolated from eight paired CNP colorectal adenocarcinoma samples. After removing low-quality cells, a total of 5,345 $CD45^+$ cells were retained for subsequent analysis. In total, 725 B cells were investigated in the present study (Figure S1), generating an average of 11.26 million uniquely mapped reads per cell. Based on this multi-regional map of the single-cell transcriptome, we provide a more comprehensive landscape of the immune microenvironment. More detailed information is discussed in our previous study.[36]

From the B cell immune atlas (Figure 1A), highly variable genes (Table S1) were used to identify cellular subtypes. We found a mature B cell subset that exhibited a $CD74^+MS4A1^+BCL11A^+CCR7^+$ phenotype (Figures 1B and 1C). In detail, CCR7 of B cells is important in the process of B cell transport to the lymph node and their maturation. B cell lymphoma 11A (*BCL11A*) is essential for B lymphoid development.[37] Furthermore, membrane spanning 4 domains A1 (MS4A1; CD20) is expressed on the surface of all B cells beginning at the pro-B phase and progressively increasing in concentration before B cell maturation. The maturation of B cells also requires the involvement of dendritic cells and macrophages for major histocompatibility complex (MHC) antigen presentation. CD74 is expressed on APCs such as macrophages, B cells, and dendritic cells. Once synthesized, CD74 is associated with MHC class II.[38,39] CD74 is a cellular receptor that is relevant for maintaining the survival of mature B cells.[40,41] It is noteworthy that the expression of genes associated with antibody production, such as *IGHG1*, *IGHG4*, *IGHA1*, and *IGHA2*, was downregulated in these B cells (Table S1). Therefore, we considered the c1 class as a group of mature B cells with a $CD74^+MS4A1^+BCL11A^+CCR7^+$ phenotype rather than plasma cells. We also observed a significant decrease in the number of these cells in tissues in the later stages of the tumor as compared to that in para-cancerous tissues. The cellular content of the para-cancerous tissue did not significantly change between stage II and III (Figure 1D).

Detection of the tipping point of B cells before lymph node metastasis in CRC

Para-cancerous tissues have a higher degree of disorder than does the cancer tissue.[6] Therefore, we hypothesized that the B cell immunity of early para-cancerous tissues undergoes more dramatic immune changes that may be useful as an early warning of CRC. Based on this hypothesis, we analyzed mature B cells in para-cancerous tissues using the DNB method (DNB analysis in Materials and methods) to locate the process of CRC metastasis.[42] The emergence of DNB indicates the arrival of a critical time point for tumor metastasis. Using the transcriptome atlas of $CD74^+CD20^+BCL11A^+CCR7^+$ B cells in the adjacent tissues of CRC at different stages of DNB analysis, we found that the peak of DNB appeared in stage II, a critical period before lymph node metastasis, where the gene network was in a period of volatile change (Figure 2A). Our results from the heatmap of DNB

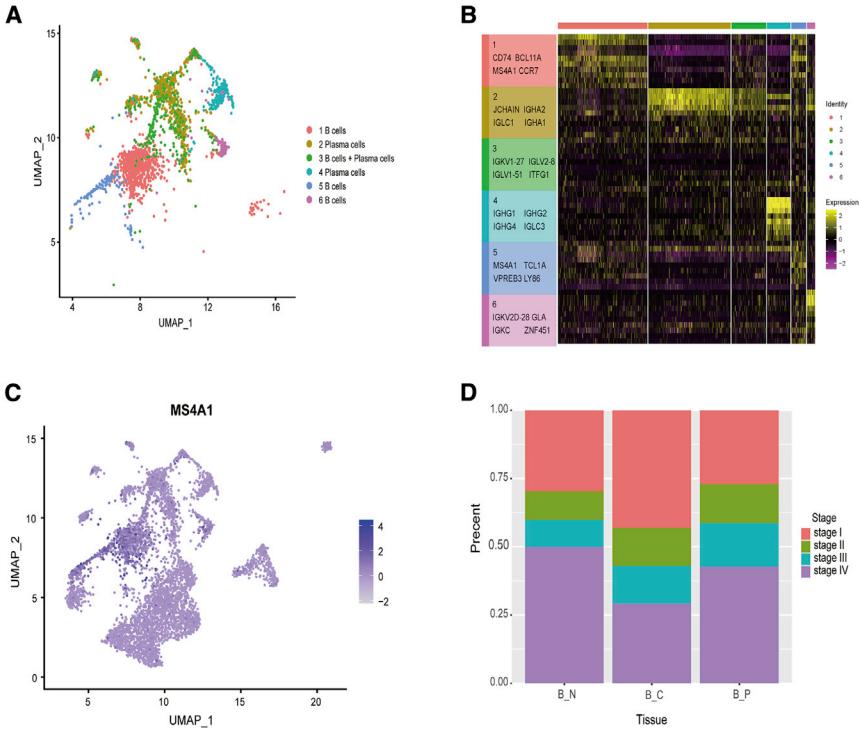

Figure 1. Colorectal cancer (CRC) B cell atlas identifies a CD74$^+$MS4A1$^+$BCL11A$^+$CCR7$^+$ B cell subtype

(A) Clustering diagram of six types of B cell subtypes after dimensionality reduction by UMAP. The figure legends represent six different types of B cells. (B) Differential heatmap of CD74$^+$MS4A1$^+$BCL11A$^+$CCR7$^+$ B cell subtypes. The list of genes on the left represents six types of cellular hypervariable genes, and the graph on the right is annotated with cell types and gene expression. (C) Specific expression of MS4A1(CD20) in CD74$^+$MS4A1$^+$ BCL11A$^+$CCR7$^+$ B cell subtypes. (D) Stacked histogram shows cell content in different tissues (CNP) at different stages.

gene clustering at different stages (I–IV) indicated a different expression pattern and a group of genes with higher expression in stage II than in other stages (Figure 2B). To further understand the dynamic changes at the gene level during metastasis progression, we classified all DNBs into four clusters using Mfuzz[43] and found that cluster 3 and cluster 4 DNB genes have high expression in stage II. This observation suggests that these genes had a vital role in stage II (Figure 2C). To understand the immune function of DNB genes at different stages, we used gene set variation analysis (GSVA) and found that most DNB genes of mature B cells were enriched in plasmacytoid dendritic cells (pDCs) and human leukocyte antigen (HLA), and they were involved in immune presentation functions (Figure 2D). In addition, the DNB genes were significantly enriched in the type 1 interferon (IFN) signaling pathway (Figure S2) related to B cell activation and antibody response.[44] Furthermore, we applied the DNB method to the B cells from the cancer tissue and found that the DNB gene number in the cancer tissue was lower than that in the para-cancerous tissue (Figure S3; Table S2). This result suggests that the para-cancerous tissue had higher dysregulation than did the cancer tissue. In summary, stage II is a critical period in CRC progression during which this subtype of B cells in the para-cancerous tissue performs essential immune functions before lymph node metastasis.

DEGs triggered by DNBs enriched in the JAK-STAT pathway involving B cell immune capability

To systematically investigate the roles of the genes overexpressed in stage II CRC (Figure 2C), we constructed a protein-protein interaction (PPI) network using the STRING database to artificially select the top 50 genes for our subsequent study. *EIF4A3*, *DHX9*, *EP300*, *STAT3*, *CCT2*, and other genes listed in the top 50 hits of the PPI network were considered as core DNB genes, suggestive of their important biological functions in B cells from CRC (Figure S4; Table S3). This was followed by a detailed study of how the DNB genes affect the first-order genes (Table S4). Thus, we used a soft clustering algorithm to classify first-order genes according to their expression trends and found that the gene expression levels of the third and fourth clusters were altered between stage II (the critical period identified by the DNB method) and stage III, but not between stage I and II (Figure S5). From the "altered genes," we selected reversed genes that were not significantly differentially expressed between stage I and II but showed significant differential expression between stage II and III (Tables S5 and S6). As a result, 129 genes were considered as reversed genes, which had variable expression over time at the network level and played an important role in the function of the identified B cell subtypes (Figure 3A; Table S7).

From the network formed by the DNB genes and its connected reversed genes (Figure 3A), two groups of genes in the inner and outer rings that were associated with the core DNB genes showed a very significant change in expression levels between stage I and III but had slight expression alterations in stage II. Seventeen of the DNB core genes were linked to the reversed genes, including the eukaryotic initiation factor (EIF) family of genes such as *EIF4E*, *EIF4A3*, and *EIF3M* and transcription factors (TFs) such as *STAT3*, *NDUFA1*, *HIF1A*, *ENO1*, and *DHX9*. The EIFs family and TFs are involved in the initiation of translation and regulation of immune-related downstream genes. These genes are involved in many immune functions such as T helper 2 cell differentiation, antigen processing, presentation of peptide antigens via MHC class I, regulation of innate immune response, and the Fc receptor signaling pathway (Figure 3B; Table 1). In summary, from stage I to stage III, stage II emerged as a critical transitional period wherein the two groups of DNB-regulated first-order interacting genes showed flipped expression. All of these genes

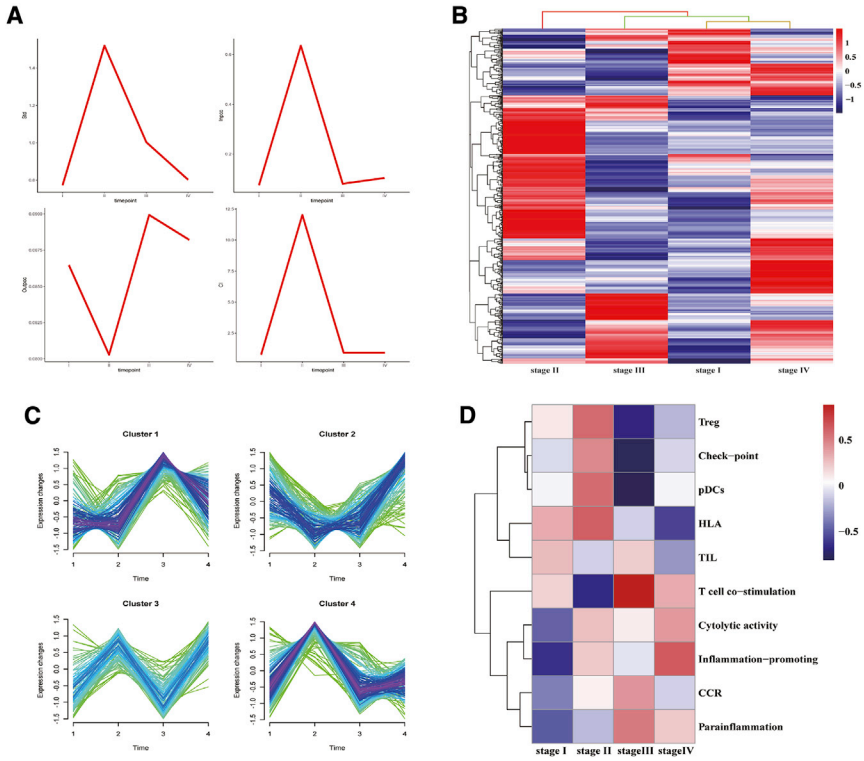

Figure 2. Detection of the tipping point of B cells before lymph node metastasis in CRC

(A) DNB shows CI peak emerges stage II. Std, standard deviation; PCC, Pearson correlation coefficient; CI, complex index. (B) Heatmap showing the expression profile of DNB genes at different stages. Hierarchical clustering showed that stage II differed from other periods in gene expression profiles. (C) DNB genes clustered by their expression pattern along the progression of CRC by the Mfuzz R package. DNB genes were classified into four clusters using soft clustering, cluster 3, cluster 4 highly expressed at stage II. (D) GSVA heatmap results show that DNB genes show different immune features at different stages. Higher ES values indicate a higher levels of enrichment to the corresponding immunophenotype for the corresponding stage. ES, enrichment score; pDC, plasmacytoid dendritic cell; HLA, human leukocyte antigen.

play important immune functions, consistent with the result of our previous DNB analysis.

As TFs are the master regulators of target gene expression, we extracted the EIFs regulatory network and the TFs regulatory network to investigate the driving role of core DNB genes. We found that 56 downstream genes among 310 DNB-reversed gene pairs were regulated by TFs, namely, *NDUFA1*, *HIF1A*, *ENO1*, *DHX9*, *ALYREF*, and *STAT3*. These genes also showed significant changes in their expression patterns between stage I and III (Figure 4A). Thus, the DNBs of upstream TFs regulate changes in DEG expression patterns. The results of Kyoto Encyclopedia of Genes and Genomes (KEGG) functional enrichment analysis showed that these genes were significantly enriched in some pathways related to immune processes, such as the JAK-STAT signaling pathway, hypoxia-inducible factor (HIF)-1 signaling pathway, and chemokine signaling pathway (Table 2). To further elaborate the role of DNBs in immune pathways, we selected JAK-STAT signaling as a significantly enriched pathway for further analysis. The JAK-STAT pathway is a prominent signaling mechanism for a series of cytokines and growth factors. STATs activate downstream cell proliferation, differentiation, migration, and apoptosis via JAK and are critical for immune development.[22] In particular, the JAK-STAT signaling pathway in B cells activates cytokines and regulates the immune system. STAT3 activates a series of downstream molecules such as protein inhibitor of activated STAT1 (PIAS1), PIAS2, suppressor of cytokine signaling 3 (SOCS3), and PIM1, which are stimulated by the extracellular immune factor interleukin (IL)-10 received from IL10RA and signaled JAK and show significantly different expression levels between stage I and III (Figure 4B). Notably, the expression of the core DNB gene, *STAT3*, did not significantly differ between stage I and III (Figure 4B). Thus, many DNB core genes act as TFs and regulate downstream genes, which undergo significant turnover between stage I and III. These turnovers imply alterations in important immune functions such as STAT3-regulated B cell development.

DHX9 in mature B cells was a specific para-cancerous prognostic biomarker

Differential expression analysis of B cells from cancer and adjacent tissues at a threshold of $p < 0.05$ revealed 5,265 DEGs (Figure S6). The result from a Wayne's diagram showed that 51 of the DNB genes were common between the CRC-adjacent and tumor tissues, and a total of 520 DNB genes were specific to the adjacent tissue (Figure S3). PPI analysis revealed the top 50 genes, and *EIF4A3*, *DHX9*, *EP300*, and *CCT2* played a hub role in the network, suggestive of their important biological functions in B cells from CRC (Figure S4). We ranked the DNB genes according to the following criteria: DEGs, network hub genes, stage II highly expressed genes, and paraneoplastic-specific DNB genes that were selected as DNB core genes. We selected six DNB core genes, *RPN1*, *NHP2*, *DHX9*, *SNRPA1*, *CCT7*, and *RAN* (Figure S7). Considering the immune function of the genes and the number of pathways, *DHX9* was considered as a para-cancer-specific DNB core gene in stage II (Figure 5A). In addition, the expression of *DHX9* tended to be high in stage II para-cancerous tissue from heatmaps of different tissues from different time periods (Figure 5B).

In stage II CRC, the high expression of *DHX9* affects the expression patterns of the surrounding genes. Several low-expression genes were affected by *DHX9* and were then overexpressed from stage II

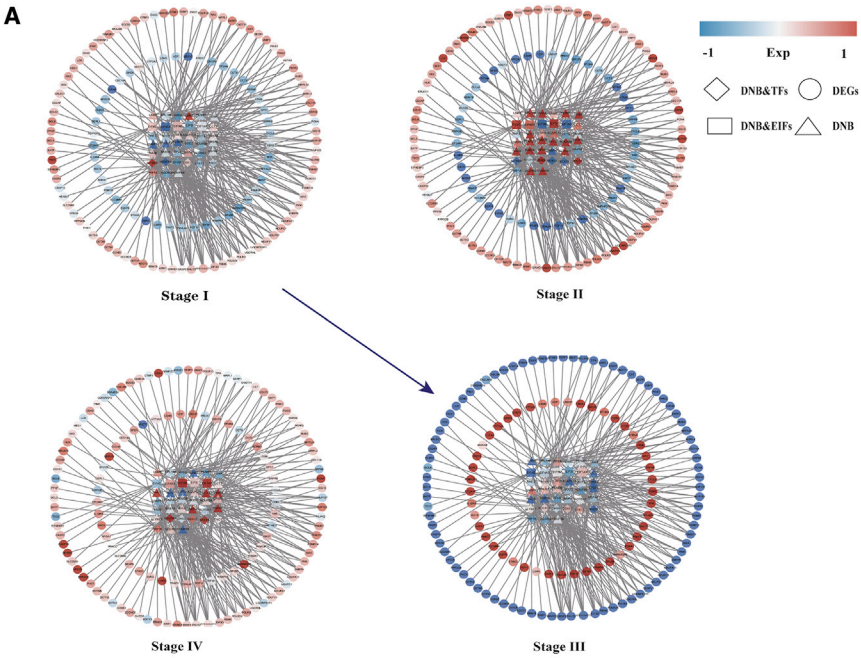

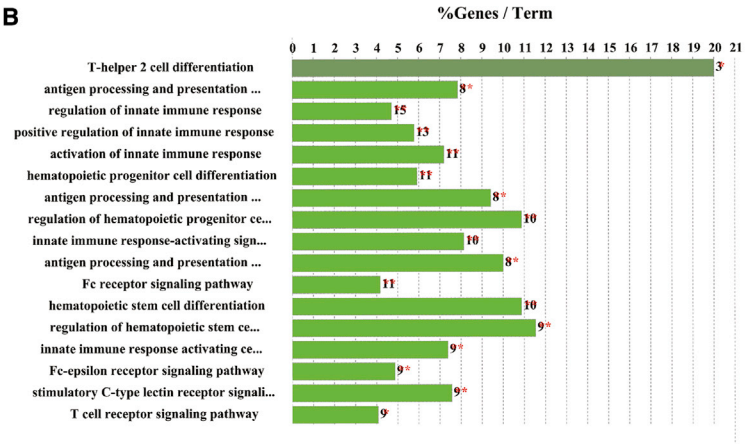

Figure 3. DNB-associated network with differentially expressed genes (DEGs) before and after a critical period

(A) DEGs in DNB-related networks before and after the critical stage. The expression of 129 DNB-associated DEGs changed significantly before (stage I) and after (stage III) the critical stage. The figure notes indicate the type of DNB genes. TF, transcription factor; EIF, translation initiation factor. (B) KEGG functional enrichment analysis of DNB network genes. %Genes/Term is the percentage of genes in a pathway, integer letters indicate the number of genes enriched, and the significance threshold is 0.05.

to III. At the same time, *DHX9* affected a large group of highly expressed genes, which were downregulated from stage II to III. Overall, *DHX9* peripheral genes showed a reversal of gene expression at the network level in stage I and III (Figure S8). To study the effects of *DHX9* and its related genes on B cell function, we performed pathway enrichment analysis and found that these genes were involved in immune function-related pathways such as TP53 pathway regulation (STRAP, CHO4), IFN, and inflammatory factors (SNRPB2) in adjacent tissue B cells, which affect CRC progression (Figure 5C; Figure S9; Table 3). This synergistic change at the network level associated with *DHX9* indicated a dramatic change in B cell molecular immune functions in the adjacent tissue. Furthermore, The Cancer Genome Atlas (TCGA) and Human Protein Atlas (HPA) analyses revealed the higher expression of *DHX9* at the RNA[45] and protein level in rectal adenocarcinoma and colon adenocarcinoma than in the normal tissue (Figure S10). To determine the efficacy of *DHX9* in clinical practice, we conducted survival analysis in patients with rectal adenocarcinoma. The results showed that *DHX9* can predict patient survival with $p < 0.05$ (Figure 5D). In summary, *DHX9* in mature B cells was a specific para-cancerous prognostic biomarker.

DISCUSSION

Mature B cells in para-cancerous tissue exhibit differential immune activity during tumor progression that may be useful to better predict early progression of CRC. Unlike differential gene expression analysis, we used the DNB method based on gene expression network modeling to predict stage II as a critical period before lymph node metastasis. We found that the antigen presentation function of this population of mature B cells was significantly enhanced in stage II. Furthermore, stage II emerged as a critical transitional period, wherein the two groups of DNB-regulated first-order interacting genes flipped their expression patterns. We found that the upstream DNB genes regulated significant changes in the expression of the downstream DEG genes. The flip-flop changes in the JAK-STAT signaling pathway between stage I and III reveal the dynamic changes in the immune functions of mature B cells. Finally, we considered *DHX9* as the core DNB gene according to the DNB ranking. *DHX9* in mature B cells is a specific para-cancerous prognostic biomarker.

In comparison with traditional methods based on the differential expression of molecular biomarkers in a static manner used to detect the metastatic state of cancers, DNB-based methods can be used to identify the pre-metastatic state during disease progression or other critical states,[46,47] with the support of dynamics-based data science.[48]

Table 1. GO analysis of DNB and its first-order network

GOID	GO term	Q value	Genes
GO:0045064	T helper 2 cell differentiation	0.01	BATF, BCL3, BCL6
GO:0002474	antigen processing and presentation of peptide antigen via MHC class I	0.00	PSMA1, PSMA2, PSMB6, PSMB7, PSMC6, PSMD12, PSMD14, PSMD8
GO:0002478	antigen processing and presentation of exogenous peptide antigen	0.00	DCTN1, DCTN3, DCTN5, PSMA1, PSMA2, PSMB6, PSMB7, PSMC6, PSMD12, PSMD14, PSMD8, RAB7A
GO:0045088	regulation of innate immune response	0.00	DHX9, HCK, HEXIM1, PIAS1, PRKCD, PSMA1, PSMA2, PSMB6, PSMB7, PSMC6, PSMD12, PSMD14, PSMD8, RPSA, SOCS3
GO:0045089	positive regulation of innate immune response	0.00	DHX9, HCK, HEXIM1, PRKCD, PSMA1, PSMA2, PSMB6, PSMB7, PSMC6, PSMD12, PSMD14, PSMD8, RPSA
GO:0002218	activation of innate immune response	0.00	HCK, HEXIM1, PRKCD, PSMA1, PSMA2, PSMB6, PSMB7, PSMC6, PSMD12, PSMD14, PSMD8
GO:0002244	hematopoietic progenitor cell differentiation	0.00	BATF, EIF2AK2, HES1, PSMA1, PSMA2, PSMB6, PSMB7, PSMC6, PSMD12, PSMD14, PSMD8
GO:0042590	antigen processing and presentation of exogenous peptide antigen via MHC class I	0.00	PSMA1, PSMA2, PSMB6, PSMB7, PSMC6, PSMD12, PSMD14, PSMD8
GO:1901532	regulation of hematopoietic progenitor cell differentiation	0.00	EIF2AK2, HES1, PSMA1, PSMA2, PSMB6, PSMB7, PSMC6, PSMD12, PSMD14, PSMD8
GO:0002758	innate immune response-activating signal transduction	0.00	HCK, PRKCD, PSMA1, PSMA2, PSMB6, PSMB7, PSMC6, PSMD12, PSMD14, PSMD8
GO:0002479	antigen processing and presentation of exogenous peptide antigen via MHC class I, TAP-dependent	0.00	PSMA1, PSMA2, PSMB6, PSMB7, PSMC6, PSMD12, PSMD14, PSMD8
GO:0038093	Fc receptor signaling pathway	0.01	HCK, PPP3CB, PRKCD, PSMA1, PSMA2, PSMB6, PSMB7, PSMC6, PSMD12, PSMD14, PSMD8
GO:0060218	hematopoietic stem cell differentiation	0.00	BATF, EIF2AK2, PSMA1, PSMA2, PSMB6, PSMB7, PSMC6, PSMD12, PSMD14, PSMD8
GO:1902036	regulation of hematopoietic stem cell differentiation	0.00	EIF2AK2, PSMA1, PSMA2, PSMB6, PSMB7, PSMC6, PSMD12, PSMD14, PSMD8
GO:0002220	innate immune response activating cell surface receptor signaling pathway	0.00	PRKCD, PSMA1, PSMA2, PSMB6, PSMB7, PSMC6, PSMD12, PSMD14, PSMD8
GO:0038095	Fcε receptor signaling pathway	0.01	PPP3CB, PSMA1, PSMA2, PSMB6, PSMB7, PSMC6, PSMD12, PSMD14, PSMD8
GO:0002223	stimulatory C-type lectin receptor signaling pathway	0.00	PRKCD, PSMA1, PSMA2, PSMB6, PSMB7, PSMC6, PSMD12, PSMD14, PSMD8
GO:0050852	T cell receptor signaling pathway	0.03	LCK, PSMA1, PSMA2, PSMB6, PSMB7, PSMC6, PSMD12, PSMD14, PSMD8

With the DNB method, calmodulin-like 3 (CALML3) was proposed as a predictive biomarker and an early warning indicator of the initiation of hepatocellular carcinoma metastasis.[29] Nitric oxide synthase 2 (NOS2) was identified as a central hub in response to cytotoxic T lymphocyte-associated protein 4 (CTLA4) blockade in cancer immune checkpoint blockade therapy.[32] These results demonstrate the feasibility of the DNB method for predicting tumor progression and immunotherapy. There are critical transitions during the EMT process, which is prevalent in paraneoplastic tissues.[31] As the adjacent colorectal tissue is also in the transitional state of the tumor tissue, we suggest a critical transition in the immune activity of mature B cells during early tumor progression, a period that facilitates early intervention.

To identify a relevant biomarker that predicts the critical pre-metastatic period of CRC, we analyzed the single-cell transcriptomic data of mature B cells with time-series properties of CRC. DNB analysis revealed that the DNB core gene *STAT3* regulated the expression of downstream genes. Furthermore, the increase in the apoptotic events of mature B cells in stage III owing to the down-regulation of downstream anti-apoptosis-related molecules could be one of the reasons for the decrease in the number of mature B cells at later stages of tumor progression.[49] In addition, *STAT3* expression was not significantly different between different periods, suggesting that it is a dark gene. Thus, its role in tumor progression is more difficult to identify using conventional methods.

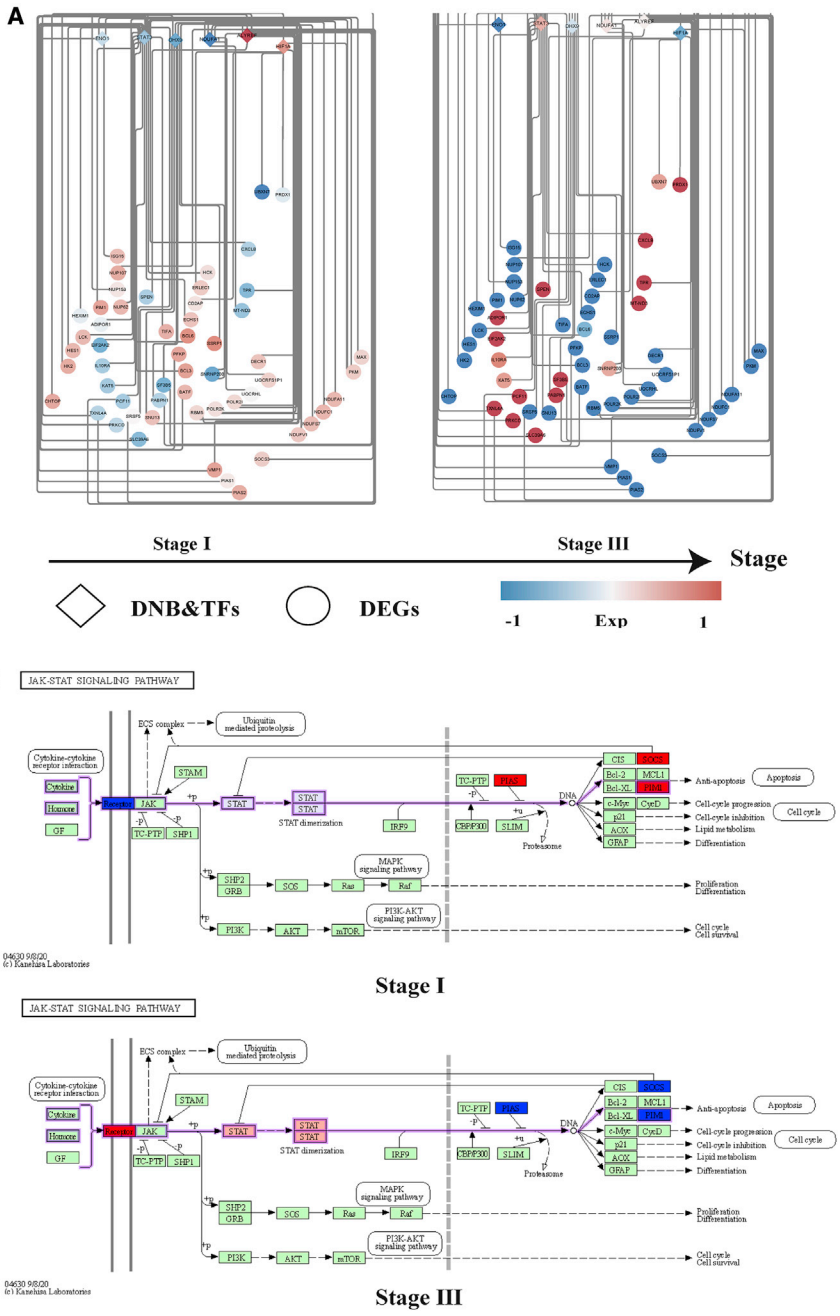

Figure 4. DEGs triggered by DNBs enriched in the JAK-STAT pathway involving B cell immune capability

(A) Transcription factor regulatory network: upstream of the DNB transcription factor, downstream of the differential gene, gene expression from low to high as from purple to red. (B) The JAK-STAT signaling pathway of B cells. Red indicates high expression; dark blue indicates low expression.

Small-molecule drugs targeting STAT3 have been developed for cancer therapy[50] and have demonstrated the potential applicability of STAT3 as an early immunotherapy target. Furthermore, we also found significant changes in the antigen presentation function of mature B cells during critical periods, suggesting that the microenvironment in the para-cancerous tissue undergoes dramatic changes at this time.[51] Thus, we can further investigate the DNB hub gene in the para-cancerous tissue through stage II where the immune changes are most dramatic.

DHX9 is an NTP-dependent RNA helicase that is non-specifically expressed in immune cells.[52,53] There have been studies reporting that DHX9 was overexpressed in CRC and promoted CRC progression.[54] DHX9 also interacts with epidermal growth factor receptor (EGFR) to activate the transcription of EGFR-responsive genes. *EGFR* is an oncogene overexpressed in several human cancers, and related drugs are widely used in the clinic.[55] Many studies have implicated DHX9 as a promoter of tumorigenesis.[56,57] However, some studies demonstrated its tumor-suppressive properties. For example, it activates target downstream genes together with the tumor suppressor *BRCA1*.[58] Moreover, its expression positively correlated with the internal ribosome entry site (IRES)-mediated up-regulation of p53 translation in response to DNA damage.[55] Knockdown of *DHX9* in lung cancer inhibits STAT3 phosphorylation and thus inhibits the EMT process in lung cancer.[59] The involvement of DHX9 in malignancies makes it an attractive biomarker and target for cancer therapy.[60] In our research, *DHX9* was overexpressed in stage II in B cells of the CRC-adjacent tissue (Figure 5B). *DHX9* and its related genes such as *STRAP, CHO4*, and *SNRPB2* exhibited a synergistic change at the network level (Figure S8). These genes are involved in TP53 pathway regulation (*STRAP*, *CHO4*),[61,62] IFN, and inflammatory factors (*EIF4A3*, *RANBP2*), and they can promote B cell activation and antibody responses. Furthermore, many reports have shown that and DHX9 activates the Toll-like receptor 4 (TLR4) signaling pathway and mediate the production of type I IFN and cellular inflammatory factors as well as innate immunity.[63] Finally, since there is synergy between DHX9 and STAT3 during the EMT process in lung cancer, our results also identified synergy between DHX9 and STAT3 at the DNB network level (Figure 3A). Thus, we are curious about the interaction with other immune cells or circulating tumor cells (CTCs)[64] in addition to the synergy of these genes in mature B cells that affect their own immune function, which may become a future

Table 2. KEGG analysis of TF regulatory network genes

Term ID	Term description	FDR	Genes
hsa00190	oxidative phosphorylation	1.04E−05	NDUFS7, NDUFV1, MT-ND3, NDUFA1, NDUFA11, NDUFC1, UQCRHL
hsa03040	spliceosome	8.90E−05	TXNL4A, SNRNP200, SF3B5, NHP2L1, ALYREF, SRSF5
hsa04714	thermogenesis	0.00015	NDUFS7, NDUFV1, MT-ND3, NDUFA1, NDUFA11, NDUFC1, UQCRHL
hsa04723	retrograde endocannabinoid signaling	0.00015	NDUFS7, NDUFV1, MT-ND3, NDUFA1, NDUFA11, NDUFC1
hsa04630	Jak-STAT signaling pathway	0.00018	IL10RA, PIAS1, STAT3, SOCS3, PIM1, PIAS2
hsa01100	metabolic pathways	0.00023	POLR2I, NDUFS7, ENO1, HK2, PKM, NDUFV1, POLR2K, MT-ND3, ECHS1, NDUFA1, PFKP, NDUFA11, NDUFC1, UQCRHL
hsa00010	glycolysis/ gluconeogenesis	0.00057	ENO1, HK2, PKM, PFKP
hsa04066	HIF-1 signaling pathway	0.0019	ENO1, STAT3, HK2, HIF1A
hsa05200	pathways in cancer	0.006	HES1, STAT3, CXCL8, MAX, TPR, PIM1, HIF1A
hsa04920	adipocytokine signaling pathway	0.0077	STAT3, SOCS3, ADIPOR1
hsa05164	influenza A	0.0096	PABPN1, EIF2AK2, CXCL8, SOCS3
hsa04062	chemokine signaling pathway	0.0121	STAT3, CXCL8, PRKCD, HCK
hsa03015	mRNA surveillance pathway	0.0127	PABPN1, PCF11, ALYREF
hsa04659	Th17 cell differentiation	0.0178	STAT3, LCK, HIF1A
hsa00052	galactose metabolism	0.0192	HK2, PFKP
hsa03020	RNA polymerase	0.0192	POLR2I, POLR2K
hsa00051	fructose and mannose metabolism	0.0195	HK2, PFKP
hsa04120	ubiquitin-mediated proteolysis	0.0306	PIAS1, SOCS3, PIAS2

research direction. In summary, DHX9 may be a potential therapeutic target for the early treatment of patients with CRC.

However, our study has some limitations. The single-cell data of CRC that we selected had only one sample in stage II. Although the cell number could meet our analysis requirement ($n > 6$), we have only a single sample for differential expression analysis. While we identified a specific $CD74^+MS4A1^+BCL11A^+CCR7^+$ B cell subtype, further validation is needed for the population of B cells using flow cytometry. In addition, it is imperative to confirm whether the DNB core genes were specifically expressed in the adjacent tissue. Finally, as we studied B cells in the adjacent tissues, we did not collect information from other relevant databases or the CRC cohort to assess the distinct prognostic value of *DHX9*. More evidence is warranted through further *in vivo* and *in vitro* studies.

In conclusion, our results from the dynamic changes in the single-cell network in CRC indicate stage II as the pre-transition stage in mature B cell functions in the adjacent tissue. The antigen-presenting and developing immune functions of this population of cells are significantly enhanced in stage II. In particular, the DEGs triggered by DNBs were enriched in the JAK-STAT pathway involving B cell immune capability. *DHX9* is a specific para-cancerous biomarker for pre-metastatic lymph nodes in CRC and a potential therapeutic target for mature B cells.

MATERIALS AND METHODS

Data

This study was approved by the local Ethics Committee of Guangdong General Hospital, Guangdong Academy of Medical Sciences (license no. 2017233H [R2]) and complied with all relevant ethical regulations.

Eight patients were recruited from Guangdong General Hospital and signed the informed consent forms (ICFs). Among these patients, two were diagnosed at stage I, one at stage II, three at stage III, and two at stage IV. For each patient, three types of fresh tissues were collected during the operation, including primary tumor tissue (C, cancer center), adjacent noncancerous tissue (P, to the brim of matched tumor 3–5 cm), and normal tissue (N, to the brim of matched tumor $\geq$10 cm). We isolated single immune cells by fluorescence-activated cell sorting (FACS) labeled by $CD45^+$ antibody and constructed Smart-Seq2 barcode libraries. The barcode libraries were sequenced using a BGISEQ500 sequencer with 100-bp single-end reads. More detailed information is discussed in our previous study.[36] After dismounting, raw reads were cleaned using Cutadapt (version 1.15) and mapped to hg38 using STAR (version 020201). Gene expression levels of each cell were quantified using RSEM (version 1.3.0) and combined in R (version 3.6.2). Cell clustering was accomplished using the R package Seurat (version 3.1.4).[65]

The data reported in this study are available in the CNGB Nucleotide Sequence Archive (CNSA: https://db.cngb.org/cnsa; accession no. CNP0000916).

B cell atlas

After quality control and filtering, the single-cell data were analyzed using Seurat (version 3.1.4). Highly variable genes were calculated using the Find Variable Genes method of the Seurat package; these genes had a mean expression value and a dispersion greater than 0.5. The selected genes were used for principal component analysis (PCA) dimension reduction on a log-normalized data matrix. The principal components were used for cluster identification at a resolution of 1.0 using the k-nearest neighbor (KNN) algorithm. We chose the uniform manifold approximation and projection (UMAP) algorithm to visualize the data.[66] Cell types from each cluster were assigned based on the expression of known cell-type markers, which were selected from the function of "FindAllMarkers" in Seurat.

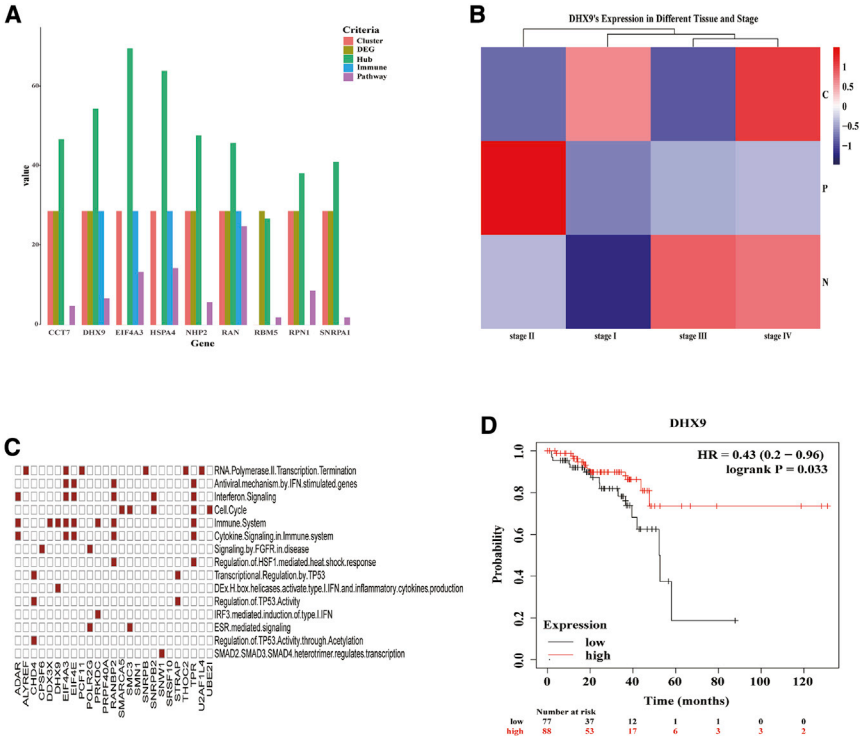

Figure 5. DHX9 in mature B cell was a specific para-cancerous prognostic biomarker

(A) We selected six DNB core genes, *RPN1, NHP2, DHX9, SNRPA1, CCT7*, and *RAN*, according to the DEG, Cluster, Hub, and PT criteria. Considering the immune function of the genes (immune) and the number of pathways (pathway), the histogram shows that *DHX9* is the most important DNB core gene. Cluster, DNB genes with high expression in stage II; Hub, the hub genes in the protein interaction network; PT, para-cancer-specific DNB genes. (B) Variation of *DHX9* gene expression in different tissues with different stages. The change from low to high gene expression is shown as a change from blue to red. C, cancerous; N, normal; P, para-cancerous. (C) The heatmap indicates the specific pathways to which *DHX9* neighboring genes are enriched. (D) Kaplan-Meier overall survival curves of *DHX9* in CRC patients (n = 165) were separated into low- and high-expression groups in terms of the median value. HR, hazard ratio; logrankP, p value of log-rank test.

DNB analysis

Before lymph node metastasis in CRC, there occurs a transition stage characterized with a dramatic change in the B cell immune activity. The change in B cell immune activity plays an important role in CRC metastasis. Thus, we applied the DNB method to identify the pre-transition stage for CRC metastasis that is primarily used to detect disease status as compared to DEG molecular biomarkers.[32] The DNB method is a new strategy to detect pre-metastasis in cancer, and it could detect a group of strongly correlated and strongly fluctuating molecules associated with early warning signals in many complex diseases. It provides a new perspective for accurately predicting CRC metastasis and uncovering potential therapeutic targets.

If the DNBs satisfied the following three criteria from the observed data, the gene network was near the critical state or tipping point: (1) for standard deviations (SDs), genes in this dominant group significantly increased; (2) Pearson's correlation coefficients (PCCs) of gene expression in this dominant (Inpcc) group significantly increased; (3) Pearson's correlation coefficients between gene expression in this group and others (Outpcc) significantly decreased; (4) CI is a complex index defined by SD, Inpcc, and Outpcc as follows: CI = (Inpcc/Outpcc)/SD, where SD is the average SD of all genes in the dominant group, Inpcc is the average PCC of all gene pairs in the dominant group (absolute value), and Outpcc is the average PCC of gene pairs between the dominant group and others (absolute value). When CI is at a peak during the time periods, the gene network is at the critical period or tipping point (Figure 2A).

Clustering

We used hierarchical clustering to cluster the DNB gene expression profiles at different times. Considering the difficulty in separating gene expression trends, we simultaneously used a more noise-robust soft clustering method (R package: Mfuzz) to cluster DNB expression profiles and first-order network gene expression profiles according to time trends, with clustering hyperparameters set to 4 and 6.[43]

GSVA

We applied GSVA to identify different stages of B cell-related immune activity.[67] We obtained 29 immune signatures represented by 29 different gene sets from the publication.[68] This annotated collection includes specific immune classifications such as various immune cell phenotypes, various immune molecules such as membrane surface antigen receptors, MHC antigens, cytokines, and antigens as well as some important immune processes. The E-values matrix was plotted as a heatmap using the R package pheatmap (version 1.0.12).

DEG identification

Differential expression analysis was performed using edgeR (version 3.28.1)[69] to identify the DEGs between different stages. Genes with a value of $q < 0.05$ and a fold change ≥ 2 were recognized as DEGs.

PPI network analysis

PPI network analysis was performed by importing the DNB gene list of B cells from CRC paraneoplastic tissue into the STRING database (version 11.0). We exported the adjacency matrix by visualizing in Cytoscape (version 3.7.1), calculating the degree of each gene using the CytoHubba plugin, and selecting the top 50 genes for visualization.

Table 3. Functional enrichment analysis of DHX9 neighboring genes

Term	Gene no.	Corrected p value	Genes
RNA polymerase II transcription termination	6	9.56E−10	ALYREF, PCF11, U2AF1L4 SNRPB, THOC2, EIF4A3
Antiviral mechanism by IFN-stimulated genes	4	6.28E−06	EIF4E, TPR, EIF4A3, RANBP2
Interferon signaling	5	6.28E−06	EIF4E, DAR, TPR, EIF4A3, RANBP2
Cell cycle	5	0.00114	UBE2I, SMC3, RANBP2, SMARCA5, TPR
Immune system	8	0.00151	DHX9, DDX3X, ADAR, PRKDC, TPR, EIF4E, EIF4A3, RANBP2
Cytokine signaling in immune system	5	0.00253	EIF4E, ADAR, TPR, nEIF4A3, RANBP2
Signaling by FGFR in disease	2	0.00432	CPSF6, POLR2G
Regulation of HSF1-mediated heat shock response	2	0.00549	TPR, RANBP2
Transcriptional regulation by TP53	3	0.01058	POLR2G, CHD4, STRAP
DEx/H-box helicases activate type I IFN and inflammatory cytokines production	1	0.01871	DHX9
Regulation of TP53 activity	2	0.02111	CHD4, STRAP
IRF3-mediated induction of type I IFN	1	0.02691	PRKDC
ESR-mediated signaling	2	0.03126	SMC3, POLR2G
Regulation of TP53 activity through Acetylation	1	0.04664	CHD4
SMAD2/SMAD3/SMAD4 heterotrimer regulates transcription	1	0.04864	SNW1

DNB core genes

The criteria we used to screen for DNB core genes were as follows: (1) PPI network analysis of genes obtained from the DNB analysis to select the gene with the highest number of connections (top 50) (hub gene); (2) selection of DNBs specific to the carcinoma relative to the DNBs of the cancerous tissue; (3) selection of highly expressed gene groups in stage II based on soft clustering analysis; and (4) differential genes. These criteria were applied together with the number of participating pathways and immune function.

Gene Ontology (GO) and pathway enrichment analysis

GO analysis is a general and useful method for annotating gene products and their characteristic functional features. GO annotation is defined into three classes (biological process, cellular component, and molecular function). The DNB gene list from CRC-adjacent tissues was used for GO analysis (ontology source: GO_ImmuneSystemProcess-EBI-UniProt). Similarly, we used Kobas (version 3.0)[70] to perform functional enrichment analysis. KEGG pathway (K) and reactome (R) were selected in the PATHWAY database options. We used a corrected p value of 0.05 as the threshold for GO annotation and significant functional enrichment. Furthermore, we also used the Cytoscape (version 3.7.1) plugin ClueGo[71] and CluePedia for pathway visualization.

TF annotation

AnimalTFDB (version 3.0) is a database designed to provide the most comprehensive and accurate information on animal TFs and cofactors, including classification and annotation of genome-wide TFs. AnimalTFDB contains 125,135 TF genes from 97 animal genomes and 8,060 transcriptional cofactor genes. To make better use of human TFs, an independent web interface to the human TF database (HumanTFDB) was designed. AnimalTFDB (version 3.0) provides comprehensive annotation and classification of TFs and cofactors and will be a useful resource for studying TFs and transcriptional regulation.[72] To further investigate the network regulatory relationships of DNB genes, this study used this database to annotate DNB core genes

Statistics and visualization

We have uploaded the expression matrix data and the reproducible analyses (R analyses) in https://github.com/Farewellznm. All data and analysis processes for this study can be found under the repository named Reproducible-DNB-downstream-analysis.

SUPPLEMENTAL INFORMATION

Supplemental information can be found online at https://doi.org/10.1016/j.omto.2021.06.004.

ACKNOWLEDGMENTS

This work was funded by grants from the Fundamental Research Funds for the Central Universities of China (no. X2SWD2172910), the Science and Technology Planning Project of Guangdong Province of China (no. 2019A030317013), the National Natural Science Foundation of China (no. 12026608), and the Guangdong Basic and Applied Basic Research Foundation (no. 2019B151502062). We thank the Guangdong Province Key Laboratory of Fermentation and Enzyme Engineering for financial support. We thank Zhong Yu for assistance with the data analysis, and Huang Yi Lin for valuable comments.

AUTHOR CONTRIBUTIONS

F.L. and R. Liu were responsible for the project administration, funding, and supervision. F.L., R. Liu, and S.L. conceived the project. H.L. and J.Z. designed the study and analyzed the data. H.L. and C.H. preprocessed the single-cell transcriptome data. P.C. and J.Z. were responsible for DNB analysis. H.L. and J.H. conducted validation and visualization analysis. H.L. was responsible for writing the manuscript. F.L., R. Li, and X.Y. contributed to the review and editing of the manuscript.

DECLARATION OF INTERESTS

The authors declare no competing interests.

REFERENCES

1. Bray, F., Ferlay, J., Soerjomataram, I., Siegel, R.L., Torre, L.A., and Jemal, A. (2018). Global cancer statistics 2018: GLOBOCAN estimates of incidence and mortality worldwide for 36 cancers in 185 countries. CA Cancer J. Clin. *68*, 394–424.
2. Arnold, M., Sierra, M.S., Laversanne, M., Soerjomataram, I., Jemal, A., and Bray, F. (2017). Global patterns and trends in colorectal cancer incidence and mortality. Gut *66*, 683–691.
3. Blackham, A.U., Swett, K., Levine, E.A., and Shen, P. (2013). Surgical management of colorectal cancer metastases to the liver: Multimodality approach and a single institutional experience. Colorectal Cancer *2*, 73–88.
4. Oh, H.H., and Joo, Y.E. (2020). Novel biomarkers for the diagnosis and prognosis of colorectal cancer. Intest. Res. *18*, 168–183.
5. Brenner, H., Kloor, M., and Pox, C.P. (2014). Colorectal cancer. Lancet *383*, 1490–1502.
6. Slaughter, D.P., Southwick, H.W., and Smejkal, W. (1953). Field cancerization in oral stratified squamous epithelium; clinical implications of multicentric origin. Cancer *6*, 963–968.
7. Li, R., Du, Y., Chen, Z., Xu, D., Lin, T., Jin, S., Wang, G., Liu, Z., Lu, M., Chen, X., et al. (2020). Macroscopic somatic clonal expansion in morphologically normal human urothelium. Science *370*, 82–89.
8. Aran, D., Camarda, R., Odegaard, J., Paik, H., Oskotsky, B., Krings, G., Goga, A., Sirota, M., and Butte, A.J. (2017). Comprehensive analysis of normal adjacent to tumor transcriptomes. Nat. Commun. *8*, 1077.
9. Sanz-Pamplona, R., Berenguer, A., Cordero, D., Mollevi, D.G., Crous-Bou, M., Sole, X., Pare-Brunet, L., Guino, E., Salazar, R., Santos, C., et al. (2014). Aberrant gene expression in mucosa adjacent to tumor reveals a molecular crosstalk in colon cancer. Mol. Cancer *13*, 46.
10. Hanahan, D., and Weinberg, R.A. (2011). Hallmarks of cancer: The next generation. Cell *144*, 646–674.
11. Markman, J.L., and Shiao, S.L. (2015). Impact of the immune system and immunotherapy in colorectal cancer. J. Gastrointest. Oncol. *6*, 208–223.
12. Havel, J.J., Chowell, D., and Chan, T.A. (2019). The evolving landscape of biomarkers for checkpoint inhibitor immunotherapy. Nat. Rev. Cancer *19*, 133–150.
13. Zappasodi, R., Merghoub, T., and Wolchok, J.D. (2018). Emerging concepts for immune checkpoint blockade-based combination therapies. Cancer Cell *33*, 581–598.
14. Lu, Y., Zhao, Q., Liao, J.Y., Song, E., Xia, Q., Pan, J., Li, Y., Li, J., Zhou, B., Ye, Y., et al. (2020). Complement signals determine opposite effects of B cells in chemotherapy-induced immunity. Cell *180*, 1081–1097.e24.
15. Sveen, A., Kopetz, S., and Lothe, R.A. (2020). Biomarker-guided therapy for colorectal cancer: Strength in complexity. Nat. Rev. Clin. Oncol. *17*, 11–32.
16. Rani, B., Cao, Y., Malfettone, A., Tomuleasa, C., Fabregat, I., and Giannelli, G. (2014). Role of the tissue microenvironment as a therapeutic target in hepatocellular carcinoma. World J. Gastroenterol. *20*, 4128–4140.
17. Mo, Z., Huang, P., Yang, C., Xiao, S., Zhang, G., Ling, F., and Li, L. (2020). Meta-analysis of 16S rRNA microbial data identified distinctive and predictive microbiota dysbiosis in colorectal carcinoma adjacent tissue. mSystems *5*, e00138-e20.
18. Varn, F.S., Wang, Y., and Cheng, C. (2018). A B cell-derived gene expression signature associates with an immunologically active tumor microenvironment and response to immune checkpoint blockade therapy. OncoImmunology *8*, e1513440.
19. De Silva, N.S., and Klein, U. (2015). Dynamics of B cells in germinal centres. Nat. Rev. Immunol. *15*, 137–148.
20. Fremd, C., Schuetz, F., Sohn, C., Beckhove, P., and Domschke, C. (2013). B cell-regulated immune responses in tumor models and cancer patients. OncoImmunology *2*, e25443.
21. Crotty, S. (2015). A brief history of T cell help to B cells. Nat. Rev. Immunol. *15*, 185–189.
22. Rawlings, J.S., Rosler, K.M., and Harrison, D.A. (2004). The JAK/STAT signaling pathway. J. Cell Sci. *117*, 1281–1283. https://doi.org/10.1242/jcs.00963.
23. Seif, F., Khoshmirsafa, M., Aazami, H., Mohsenzadegan, M., Sedighi, G., and Bahar, M. (2017). The role of JAK-STAT signaling pathway and its regulators in the fate of T helper cells. Cell Commun. Signal. *15*, 23.
24. Guo, F.F., and Cui, J.W. (2019). The role of tumor-infiltrating B cells in tumor immunity. J. Oncol. *2019*, 2592419.
25. Zhou, M., Zhang, Z., Bao, S., Hou, P., Yan, C., Su, J., and Sun, J. (2021). Computational recognition of lncRNA signature of tumor-infiltrating B lymphocytes with potential implications in prognosis and immunotherapy of bladder cancer. Brief. Bioinform. *22*, bbaa047.
26. Raman, D., Baugher, P.J., Thu, Y.M., and Richmond, A. (2007). Role of chemokines in tumor growth. Cancer Lett. *256*, 137–165. https://doi.org/10.1016/j.canlet.2007.05.013.
27. Le, Y., Zhou, Y., Iribarren, P., and Wang, J. (2004). Chemokines and chemokine receptors: Their manifold roles in homeostasis and disease. Cell. Mol. Immunol. *1*, 95–104.
28. Harwood, N.E., and Batista, F.D. (2010). Antigen presentation to B cells. F1000 Biol. Rep. *2*, 87.
29. Yang, B.W., Li, M.Y., Tang, W.Q., Liu, W.X., Zhang, S., Chen, L.N., and Xia, J.L. (2018). Dynamic network biomarker indicates pulmonary metastasis at the tipping point of hepatocellular carcinoma. Nat Commun *9*, 678.
30. Chen, P., Chen, E., Chen, L., Zhou, X.J., and Liu, R. (2019). Detecting early-warning signals of influenza outbreak based on dynamic network marker. J. Cell. Mol. Med. *23*, 395–404.
31. Jiang, Z.L., Lu, L.N., Liu, Y.W., Zhang, S., Li, S.X., Wang, G.Y., Wang, P., and Chen, L.N. (2020). SMAD7 and SERPINE1 as novel dynamic network biomarkers detect and regulate the tipping point of TGF-beta induced EMT. Sci. Bull. (Beijing) *65*, 842–853.
32. Lesterhuis, W.J., Bosco, A., Millward, M.J., Small, M., Nowak, A.K., and Lake, R.A. (2017). Dynamic versus static biomarkers in cancer immune checkpoint blockade: Unravelling complexity. Nat. Rev. Drug Discov. *16*, 264–272.
33. Liu, R., Wang, J., Ukai, M., Sewon, K., Chen, P., Suzuki, Y., Wang, H., Aihara, K., Okada-Hatakeyama, M., and Chen, L. (2019). Hunt for the tipping point during endocrine resistance process in breast cancer by dynamic network biomarkers. J. Mol. Cell Biol. *11*, 649–664.
34. Liu, R., Chen, P., and Chen, L. (2020). Single-sample landscape entropy reveals the imminent phase transition during disease progression. Bioinformatics *36*, 1522–1532.
35. Liu, R., Aihara, K., and Chen, L. (2021). Collective fluctuation implies imminent state transition: Comment on "Dynamic and thermodynamic models of adaptation" by A.N. Gorban et al. Phys. Life Rev. *37*, 103–107.
36. Wang, W., Zhong, Y., Zhuang, Z., Xie, J., Lu, Y., Huang, C., Sun, Y., Wu, L., Yin, J., Yu, H., et al. (2021). Multiregion single-cell sequencing reveals the transcriptional landscape of the immune microenvironment of colorectal cancer. Clin. Transl. Med. *11*, e253.
37. Yu, Y., Wang, J., Khaled, W., Burke, S., Li, P., Chen, X., Yang, W., Jenkins, N.A., Copeland, N.G., Zhang, S., and Liu, P. (2012). Bcl11a is essential for lymphoid development and negatively regulates p53. J. Exp. Med. *209*, 2467–2483.
38. Henne, C., Schwenk, F., Koch, N., and Möller, P. (1995). Surface expression of the invariant chain (CD74) is independent of concomitant expression of major histocompatibility complex class II antigens. Immunology *84*, 177–182.
39. Ong, G.L., Goldenberg, D.M., Hansen, H.J., and Mattes, M.J. (1999). Cell surface expression and metabolism of major histocompatibility complex class II invariant chain (CD74) by diverse cell lines. Immunology *98*, 296–302.
40. Gil-Yarom, N., Radomir, L., Sever, L., Kramer, M.P., Lewinsky, H., Bornstein, C., Blecher-Gonen, R., Barnett-Itzhaki, Z., Mirkin, V., Friedlander, G., et al. (2017). CD74 is a novel transcription regulator. Proc. Natl. Acad. Sci. USA *114*, 562–567.
41. Cohen, S., and Shachar, I. (2012). Cytokines as regulators of proliferation and survival of healthy and malignant peripheral B cells. Cytokine *60*, 13–22.
42. Liu, R., Li, M., Liu, Z.P., Wu, J., Chen, L., and Aihara, K. (2012). Identifying critical transitions and their leading biomolecular networks in complex diseases. Sci. Rep. *2*, 813.
43. Kumar, L., and Futschik, M.E. (2007). Mfuzz: A software package for soft clustering of microarray data. Bioinformation *2*, 5–7.
44. McNab, F., Mayer-Barber, K., Sher, A., Wack, A., and O'Garra, A. (2015). Type I interferons in infectious disease. Nat. Rev. Immunol. *15*, 87–103.

45. Chandrashekar, D.S., Bashel, B., Balasubramanya, S.A.H., Creighton, C.J., Ponce-Rodriguez, I., Chakravarthi, B.V.S.K., and Varambally, S. (2017). UALCAN: A portal for facilitating tumor subgroup gene expression and survival analyses. Neoplasia *19*, 649–658.

46. Liu, R., Zhong, J., Hong, R., Chen, E., Aihara, K., Chen, P., and Chen, L. (2021). Predicting local COVID-19 outbreaks and infectious disease epidemics based on landscape network entropy. Sci. Bull. (Beijing). https://doi.org/10.1016/j.scib.2021.03.022.

47. Zhong, J., Liu, R., and Chen, P. (2020). Identifying critical state of complex diseases by single-sample Kullback-Leibler divergence. BMC Genomics *21*, 87.

48. Chen, P., Liu, R., Aihara, K., and Chen, L. (2020). Autoreservoir computing for multistep ahead prediction based on the spatiotemporal information transformation. Nat. Commun. *11*, 4568.

49. Bauer, K., Binder, S., Klein, C., Simon, J.C., and Horn, F. (2009). Inhibition of dendritic cell maturation and activation is mediated by STAT3. Cell Commun. Signal. *7* (*Suppl 1*), A68.

50. Schust, J., Sperl, B., Hollis, A., Mayer, T.U., and Berg, T. (2006). Stattic: A small-molecule inhibitor of STAT3 activation and dimerization. Chem. Biol. *13*, 1235–1242.

51. Burrows, P.D., and Cooper, M.D. (1997). B cell development and differentiation. Curr. Opin. Immunol. *9*, 239–244.

52. Zhang, Z., Yuan, B., Lu, N., Facchinetti, V., and Liu, Y.J. (2011). DHX9 pairs with IPS-1 to sense double-stranded RNA in myeloid dendritic cells. J. Immunol. *187*, 4501–4508.

53. Kim, T., Pazhoor, S., Bao, M., Zhang, Z., Hanabuchi, S., Facchinetti, V., Bover, L., Plumas, J., Chaperot, L., Qin, J., and Liu, Y.J. (2010). Aspartate-glutamate-alanine-histidine box motif (DEAH)/RNA helicase A helicases sense microbial DNA in human plasmacytoid dendritic cells. Proc. Natl. Acad. Sci. USA *107*, 15181–15186.

54. Hou, P., Meng, S., Li, M., Lin, T., Chu, S., Li, Z., Zheng, J., Gu, Y., and Bai, J. (2021). LINC00460/DHX9/IGF2BP2 complex promotes colorectal cancer proliferation and metastasis by mediating HMGA1 mRNA stability depending on m6A modification. J. Exp. Clin. Cancer Res. *40*, 52.

55. Lee, T., and Pelletier, J. (2016). The biology of DHX9 and its potential as a therapeutic target. Oncotarget *7*, 42716–42739.

56. Ding, X., Jia, X., Wang, C., Xu, J., Gao, S.J., and Lu, C. (2019). A DHX9-lncRNA-MDM2 interaction regulates cell invasion and angiogenesis of cervical cancer. Cell Death Differ. *26*, 1750–1765.

57. Cao, S., Sun, R., Wang, W., Meng, X., Zhang, Y., Zhang, N., and Yang, S. (2017). RNA helicase DHX9 may be a therapeutic target in lung cancer and inhibited by enoxacin. Am. J. Transl. Res. *9*, 674–682.

58. Anderson, S.F., Schlegel, B.P., Nakajima, T., Wolpin, E.S., and Parvin, J.D. (1998). BRCA1 protein is linked to the RNA polymerase II holoenzyme complex via RNA helicase A. Nat. Genet. *19*, 254–256.

59. Cristini, A., Groh, M., Kristiansen, M.S., and Gromak, N. (2018). RNA/DNA hybrid interactome identifies DXH9 as a molecular player in transcriptional termination and R-loop-associated DNA damage. Cell Rep. *23*, 1891–1905.

60. Gulliver, C., Hoffmann, R., and Baillie, G.S. (2020). The enigmatic helicase DHX9 and its association with the hallmarks of cancer. Future Sci. OA *7*, FSO650.

61. Yu, L., Yu, T.T., and Young, K.H. (2019). Cross-talk between Myc and p53 in B-cell lymphomas. Chronic Dis. Transl. Med. *5*, 139–154.

62. Seong, H.A., Manoharan, R., and Ha, H. (2011). B-MYB positively regulates serine-threonine kinase receptor-associated protein (STRAP) activity through direct interaction. J. Biol. Chem. *286*, 7439–7456.

63. Ng, Y.C., Chung, W.C., Kang, H.R., Cho, H.J., Park, E.B., Kang, S.J., and Song, M.J. (2018). A DNA-sensing-independent role of a nuclear RNA helicase, DHX9, in stimulation of NF-κB-mediated innate immunity against DNA virus infection. Nucleic Acids Res. *46*, 9011–9026.

64. Wei, C., Yang, C., Wang, S., Shi, D., Zhang, C., Lin, X., Liu, Q., Dou, R., and Xiong, B. (2019). Crosstalk between cancer cells and tumor associated macrophages is required for mesenchymal circulating tumor cell-mediated colorectal cancer metastasis. Mol. Cancer *18*, 64.

65. Butler, A., Hoffman, P., Smibert, P., Papalexi, E., and Satija, R. (2018). Integrating single-cell transcriptomic data across different conditions, technologies, and species. Nat. Biotechnol. *36*, 411–420.

66. Becht, E., McInnes, L., Healy, J., Dutertre, C.A., Kwok, I.W.H., Ng, L.G., Ginhoux, F., and Newell, E.W. (2019). Dimensionality reduction for visualizing single-cell data using UMAP. Nat. Biotechnol. *37*, 38–44.

67. Hanzelmann, S., Castelo, R., and Guinney, J. (2013). GSVA: Gene set variation analysis for microarray and RNA-seq data. BMC Bioinformatics *14*, 7.

68. He, Y., Jiang, Z., Chen, C., and Wang, X. (2018). Classification of triple-negative breast cancers based on immunogenomic profiling. J. Exp. Clin. Cancer Res. *37*, 327.

69. Robinson, M.D., McCarthy, D.J., and Smyth, G.K. (2010). edgeR: A Bioconductor package for differential expression analysis of digital gene expression data. Bioinformatics *26*, 139–140.

70. Xie, C., Mao, X., Huang, J., Ding, Y., Wu, J., Dong, S., Kong, L., Gao, G., Li, C.Y., and Wei, L. (2011). KOBAS 2.0: A web server for annotation and identification of enriched pathways and diseases. Nucleic Acids Res. *39*, W316–W322.

71. Bindea, G., Mlecnik, B., Hackl, H., Charoentong, P., Tosolini, M., Kirilovsky, A., Fridman, W.H., Pagès, F., Trajanoski, Z., and Galon, J. (2009). ClueGO: A Cytoscape plug-in to decipher functionally grouped gene ontology and pathway annotation networks. Bioinformatics *25*, 1091–1093.

72. Hu, H., Miao, Y.R., Jia, L.H., Yu, Q.Y., Zhang, Q., and Guo, A.Y. (2019). AnimalTFDB 3.0: A comprehensive resource for annotation and prediction of animal transcription factors. Nucleic Acids Res. *47* (D1), D33–D38.